Respirology (2007) 12, 856–862 doi: 10.1111/j.1440-1843.2007.01158.x

ORIGINAL ARTICLE

Development and validation of diagnostic prediction model for solitary pulmonary nodules

KAN YONEMORI,[1] UKIHIDE TATEISHI,[1] HAJIME UNO,[2] YOKO YONEMORI,[3] KOJI TSUTA,[4] MASAHIRO TAKEUCHI,[2] YOSHIHIRO MATSUNO,[4] YASUHIRO FUJIWARA,[5] HISAO ASAMURA[6] AND MASAHIKO KUSUMOTO[1]

Divisions of [1]Diagnostic Radiology and [4]Clinical Laboratory, [5]Medical Oncology Division and [6]Thoracic Surgery Division, National Cancer Center Hospital, [2]Division of Biostatistics, School of Pharmaceutical Sciences, Kitasato University, Tokyo, and [3]Department of Basic Pathology, Graduate School of Medicine, Chiba University, Chiba, Japan

Development and validation of diagnostic prediction model for solitary pulmonary nodules
YONEMORI K, TATEISHI U, UNO H, YONEMORI Y, TSUTA K, TAKEUCHI M, MATSUNO Y, FUJIWARA Y, ASAMURA H, KUSUMOTO M. *Respirology* 2007; **12**: 856–862

Background and objective: The aim of this study was to develop a simple prediction model for the underlying diagnosis of solitary pulmonary nodules (SPN) based on clinical characteristics and thin-section CT findings.

Methods: Retrospective analysis was carried out on 452 patients with SPN (113 benign and 339 malignant) smaller than 30 mm, who underwent thin-section CT followed by surgical resection and histological diagnosis. The clinical characteristics were collected from medical records, and radiographic characteristics from thin-section CT findings. The prediction model was determined using multivariate logistic analysis. The prediction model was validated in 148 consecutive patients with undiagnosed SPN, and the diagnostic accuracy of the model was compared with that of an experienced chest radiologist.

Results: The prediction model comprised the level of serum CRP, the level of carcinoembryonic antigen, the presence or absence of calcification, spiculation and CT bronchus sign. The areas under the receiver-operating characteristic curve in training and validation sets were 0.966 and 0.840, respectively. The diagnostic accuracies of the prediction model and the experienced chest radiologist for the validation set were 0.858 and 0.905, respectively.

Conclusion: The simple prediction model consisted of two biochemical and three radiographic characteristics. The diagnostic accuracy of an experienced chest radiologist was higher compared with the prediction model.

Key words: benign, CT, malignant, prediction model, solitary pulmonary nodule.

INTRODUCTION

The prevalence of a solitary pulmonary nodule (SPN), discovered on a CXR or CT scan, is reportedly 0.09 to 0.20% for all chest radiographs.[1,2] Most SPNs are benign, but malignancy accounts for approximately 20% of SPN, with a range of 3–80%.[3–5]

Although the diagnosis of an SPN may require resection, physicians should, as far as possible, minimize the risk of unnecessary surgery, especially in patients with benign diseases. Most physicians attempt to distinguish benign from malignant nodules using CXR, CT scanning, PET scans and fine-needle aspiration. Recent advances in radiographic

Correspondence: Kan Yonemori, Division of Diagnostic Radiology, National Cancer Center Hospital, 5-1-1 Tsukiji, Chuo-ku, Tokyo 104-0045, Japan. Email: kyonemor@ncc.go.jp

Presented in part at the 100th American Thoracic Society International Conference, San Diego, USA, 20–25 May 2005.

Received 24 November 2006; invited to revise 20 December 2006 and 28 January 2007; revised 23 December 2006 and 15 February 2007; accepted 5 March 2007 (Associate Editor: Yoichi Nakanishi).

modalities and technology have improved the physicians' ability to assess the SPN, using information such as margin patterns, size, growth rate and location. Diagnostic and treatment decisions depend on the physician's assessment of the probability of malignancy of each SPN.

Improving the diagnostic accuracy of SPN in individual patients is a challenge. Previous methods for estimating the likelihood of each diagnosis used either Bayesian statistics or multivariate logistic regression analysis.[5–9] A Bayesian statistical model estimates the likelihood ratios by measuring the probability of finding a given feature in a population with malignant SPNs and dividing that by the probability of finding the same feature in a population with benign SPNs.[6,7] A certain scepticism regarding the Bayesian approach exists, and these models are not often applied in Western countries.[9] After the advent of CT scanning, Swensen *et al.* reported a multivariate logistic model that incorporated patient age, smoking history, a history of extra-thoracic malignancy, diameter, upper lobe location of the SPN, and the presence or absence of spiculation.[8]

Serum tumour markers are associated with malignancy.[10] No study has analysed the role of biochemical markers in differentiating between malignant and benign SPNs, and whether it may improve the performance of a prediction model. The aim of this study was to develop a simple prediction model for the diagnosis of SPN, based on clinical characteristics and thin-section CT findings, and to evaluate its diagnostic accuracy compared with that of an experienced chest radiologist.

METHODS

Records of 452 patients with SPNs who underwent surgery because of suspicion of primary lung cancer between July 1998 and March 2004 were retrieved (the training set: 113 benign SPNs, 339 malignant SPNs). All resected SPNs were evaluated histologically and a diagnosis made. Inclusion criteria were an SPN which was a solitary, round or oval lesion ≤30 mm in diameter and without associated adenopathy, atelectasis or effusion.[11] Any SPN diagnosed as metastatic extrapulmonary cancer was excluded. Benign SPN was defined as a benign pathological diagnosis. Malignant SPN was defined as that caused by primary lung cancer, such as non-small-cell or small-cell lung cancer. This study was approved by the institutional review board after confirmation of informed consent by the patient to have records and images reviewed.

The CT scans were acquired on single helical or multidetector scanners (X-Vigor, or Aquilion, Toshiba Medical Systems, Tokyo, Japan). The helical technique in all patients consisted of 10.0-mm collimation for individual scans of the entire lung (120 kVp, 150–200 mA) and reconstruction by a standard algorithm prior to surgery. In all patients, additional thin-section CT images were obtained with 2.0-mm collimation, a 20-cm field of view, 120 kVp and 200 mA per rotation, 0.5- or 1.0-s gantry rotation, and a high-spatial-frequency reconstruction algorithm. Hardcopy images were photographed at window settings for the lung (centre: –600 HU and width: 2000 HU) and mediastinum (centre: 50 HU and width: 550 HU).

Development of the prediction model

The clinical characteristics of patients comprising the training set ($n = 452$) were collected from the medical records: gender, age, smoking status (current or former smoker), history of extra-thoracic malignancies (>5 years previously), blood count and blood chemistry, including WCC, CRP, and serum tumour markers: carcinoembryonic antigen (CEA), sialyl-specific embryonic antigen, cytokeratin 19 fragment, squamous-cell carcinoma antigen, carbohydrate antigen 19–9, neurone-specific enolase and progastrin-releasing peptide. Two observers (K.Y., S.T.), blind to the clinical or histopathological diagnoses, reviewed the thin-section CT images, and the final decisions on diagnosis were reached by consensus. Thin-section CT findings of SPN in the training set were reviewed as follows: lung side (right vs left), location (lobe), diameter (mm), the presence or absence of calcification, cavity, lobulation, spiculation and CT bronchus sign. The CT bronchus sign was defined as a visible bronchus or bronchiolus leading to the SPN.[12]

Categorical variables of clinical characteristics and thin-section CT findings were compared using the chi-square test. Continuous variables were compared using the *t*-test. The prediction model was identified from multivariate logistic regression analysis. A stepwise procedure was used to select independent variables from the statistically significant variables in univariate analysis. Continuous variables in serum tumour markers without complete data sets were excluded from the logistic regression analysis. Some functional forms for continuous variables were also explored in the logistic regression analysis. The Hosemer-Lemeshow test was performed to evaluate goodness-of-fit of the prediction model. The performance of the prediction model was evaluated by calculating the prediction accuracy, the receiver-operating characteristic (ROC) curve and area under the curve. The statistical analysis was performed with SAS version 8.2 (SAS Institute, Cary, NC, USA), and the significance level was set at 0.05 (two-sided).

Validation of the prediction model

The prediction model was validated by comparing its accuracy with that of an experienced chest radiologist in the validation set. The validation set comprised a consecutive series of 148 patients with undiagnosed SPNs, who underwent thin-section CT imaging prior to surgery, between May 2004 and April 2005. The resected SPN was diagnosed pathologically as benign or malignant.

The reviews of thin-section CT images were performed independently before surgery. An observer (U.T.) reviewed the radiological predictive factors for

Table 1 Comparison of the clinical and radiological characteristics of the patients diagnosed with a benign or malignant solitary pulmonary nodule in the training set

Classification	Benign (n = 113)	Malignant (n = 339)	Total (N = 452)	P-value*
Clinical characteristics				
Male (%)	54	56	55	0.70
Mean age (years)	58	64	62	0.002
Current or past smoker (%)	47	54	49	0.86
Mean pack-years (n)	19	24	23	0.59
Other cancer >5 years ago (%)	11	10	10	0.79
Mean WCC ($\times 10^9$/L)	6.27	6.33	6.31	0.41
Mean serum CRP (mg/L)	1.0	3.0	2.0	<0.001
Mean serum CEA (ng/mL)	2.7	5.6	4.9	<0.001
Radiological characteristics				
Mean diameter (mm)	17	20	19	0.02
Side (right) (%)	65	63	64	0.65
Location (%)				
LUL	11	17	15	0.14
Lingular segment	5	5	5	0.80
LLL	18	14	15	0.37
RUL	30	31	31	0.91
RML	13	9	10	0.21
RLL	22	22	22	0.99
Calcification (%)	12	2	5	<0.001
Cavitation (%)	10	8	8	0.49
Lobulation (%)	16	12	13	0.26
Spiculation (%)	2	84	63	<0.001
CT bronchus sign (%)	32	82	69	<0.001

*Univariate analysis: chi-squared test and t-tests were performed for proportional differences or mean differences in variables between benign and malignant SPNs.

CEA, carcinoembryonic antigen; LLL, left lower lobe; LUL, left upper lobe; RLL, right lower lobe; RML, right middle lobe; RUL, right upper lobe.

the prediction models in the thin-section CT images. An experienced chest radiologist (M.K.) reviewed the thin-section CT images with no knowledge of either the clinical data or the present prediction model. This experienced chest radiologist evaluated prediction of an SPN on a 5-point scale, scored as follows: 1, benign; 2, probably benign; 3, indeterminate; 4, probably malignant; and 5, malignant. He then determined a diagnosis (malignant or benign SPNs). Based on the pathological diagnosis, all SPNs were divided into benign or malignant for the purpose of evaluation of the validation set.

RESULTS

The clinical and the radiological characteristics of the 452 patients in the training set (113 benign SPNs, 339 malignant SPNs) are presented in Table 1.

Sixty-three per cent of the benign SPNs were granulomas, and the remainder included sclerosing haemangioma and hamartoma. The majority of the malignant SPNs were adenocarcinoma of the lung (80.2%). Other malignancies included squamous-cell carcinoma (14.5%), large-cell carcinoma (3.5%), adenosquamous carcinoma (0.3%), adenoid cystic carcinoma (0.3%), neuroepidermoid carcinoma (0.3%) and small-cell lung carcinoma (0.9%).

The SPN prediction model defined the probability of benign SPN as follows: Probability of benign SPN = $e^x/(1+e^x)$, $x = 3.7009 + (3.0705 \times \text{calcification}) + (-1.3243 \times \text{CT bronchus sign}) + (-5.3399 \times \text{spiculation}) + (-1.16 \times \sqrt{\text{CEA}}) + (-1.4987 \times \sqrt{\text{CRP}})$, e is the base of natural logarithms. Calcification = 1 if calcification is present in the SPN (otherwise = 0); CT bronchus sign = 1 if CT bronchus sign is present (otherwise = 0); spiculation = 1 if spiculated appearance is present (otherwise = 0); CEA = serum CEA level (ng/mL); CRP = serum CRP level (mg/L). The area under ROC in the training set was 0.966 (Fig. 1). The goodness-of-fit statistic, as described by Hosmer-Lemeshow, for the derivation dataset was $\chi^2 = 11.608$, P-value = 0.170. If the biological parameters were not available, the alternative prediction model was as follows: Probability of benign SPN = $e^x/(1+e^x)$, $x = 1.084 + (2.7851 \times \text{calcification}) + (-1.1795 \times \text{CT bronchus sign}) + (-5.4481 \times \text{spiculation})$. The area under ROC of the alternative prediction model in the training set was 0.94.

Following derivation of the prediction model, a further 148 patients with a newly discovered indeterminate SPN were identified between May 2004 and

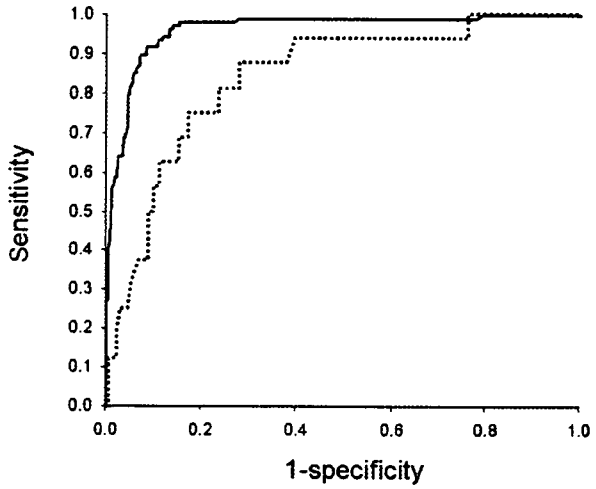

Figure 1 Receiver-operating characteristic curve for the prediction model for the diagnosis of a solitary pulmonary nodule (SPN) (solid line). The prediction model was developed based on data from 452 patients with a solitary pulmonary nodule. Receiver-operating characteristic curve for the prediction model when validated in 148 consecutive patients with SPNs (dotted line).

April 2005 (the validation set). The differences in the clinical and radiological characteristics of both sets are presented in Table 2.

Eighty-nine per cent of the validation set had malignant SPNs, and the reminder benign SPNs. Forty-seven per cent of the benign SPNs were granulomas; other diagnoses included sclerosing haemangioma, hamartoma, fibrosis, organizing pneumonia and inflammation. The majority of the malignant SPNs were adenocarcinoma of the lung (88%); other malignancies included squamous-cell carcinoma (7.4%), large-cell carcinoma (2.7%), pleomorphic carcinoma (0.7%), small-cell lung carcinoma (0.7%), and mucosa-associated lymphoid tissue (MALT) lymphoma of the lung (0.7%). The respective mean serum CEA and CRP levels in benign SPNs were 3.1 ng/mL (range 0.8–16.7) and 1.0 mg/L (range 1.0–3.0). The corresponding mean serum CEA and CRP levels in malignant SPNs were 5.1 ng/mL (range 0.5–58.4) and 3.0 mg/L (range 1.0–165). The mean diameters of the benign and malignant SPNs were 16 mm (range 10–23) and 17 mm (range 8–30), respectively.

In the validation set ($n = 148$), the area under ROC of the prediction model was 0.84 (Fig. 1), and the accuracies of the prediction model and the experienced chest radiologist were 0.858 and 0.905, respectively. ROC and accuracy of the alternative prediction model were 0.81 and 0.75. The experienced chest radiologist's prediction was inconsistent with 59% of benign SPNs, and 4% of malignant SPNs (3: adenocarcinoma; 1: pleomorphic carcinoma; 1: MALT of the lung).

DISCUSSION

This study has demonstrated a simple prediction model for the diagnosis of SPN based on two clinical variables and three radiological variables using thin-section CT findings. The accuracy of the prediction model was demonstrated to be high in a validation based on consecutive patients with undiagnosed SPNs, although not as high as the accuracy of the experienced chest radiologist's diagnostic prediction.

Statistical analysis indicated two biochemical markers for inclusion in the prediction model, but did not include the patient characteristics of age, cigarette-smoking status and past history of extra-pulmonary malignancy.[8] The frequency of a malignant SPN rises with increasing patient age. In the present study, age was significantly associated with a malignant SPN on univariate analysis. Several studies have reported the frequency of malignant SPN to be more than 50% higher in patients aged 50 years and over than in those aged less than 50 years.[13] Similarly, cigarette-smoking and past history of extra-pulmonary malignancy reportedly have strong associations with lung cancer or malignant SPNs. The training and validation sets included 9% and 6% of patients less than 50 years of age, respectively. Although the mean age and frequency of past history of extra-pulmonary malignancy in this study were similar to those in the previously reported prediction model, the frequency of cigarette smoking in this study was slightly lower than the 68% of patients with SPNs in the previous study.[9] According to data from Japan Tobacco Industry, Inc., the overall smoking prevalences in men and women were 57.5% and 14% in 1996 respectively, which are significantly different from the prevalence in the 1960s.[14] These patients' demographic characteristics varied from the frequencies in other SPN reports, possibly influenced by the role of the institution involved, the period or the patient population.

Serum markers based on tumour biology would not have been strongly influenced by patient population or institution. CEA is a marker for a wide range of malignancies, including lung cancer. Elevation of serum CEA was found in 16% to 27% of patients with clinical stage IA non-small-cell lung cancer.[15,16] Although the serum CEA level was associated with cigarette smoking and age,[17] the multivariate analysis used to develop the prediction model indicated the significance of serum CEA rather than these known confounding factors included in the previous prediction model.

CRP, an acute-phase protein synthesized in hepatocytes, is up-regulated by cytokines, such as IL-6 and tumour necrosis factor-α.[18,19] Increased serum CRP levels have also been recognized as part of a paraneoplastic syndrome for several malignant tumours, including lung cancer.[20] In addition, serum CRP was significantly higher in patients with lung cancer than in those with benign lung disease or the healthy population.[21–23] The laboratory variables in the prediction model were supported by these previous studies and our results; that is, the serum markers in patients with malignant SPNs were both higher than in those with benign SPNs. CT has been shown to be an effective means of morphologically differentiating benign from malignant SPNs. Numerous studies have described the radiographic characteristics of SPN,

Table 2 Comparison of the clinical and radiological characteristics in both training and validation patient sets

	Training set ($n = 452$)	Validation set ($n = 148$)	*P*-value*
Clinical characteristics			
Male (%)	56	57	0.69
Mean age (years)	62	63	0.82
Current or past smoker (%)	49	50	0.82
Other cancer >5 years ago (%)	10	11	0.60
Mean serum CEA (ng/mL)	4.9	4.9	0.99
Mean serum CRP (mg/L)	2.0	3.0	0.56
Radiological characteristics			
Mean diameter (mm)	19	17	<0.01
Side (right) (%)	64	61	0.63
Location (%)			
LUL	15	20	0.15
Lingular segment	5	2	0.13
LLL	15	16	0.73
RUL	31	32	0.74
RML	10	7	0.32
RLL	22	22	0.85
Calcification (%)	5	0	<0.01
Spiculation (%)	63	68	0.27
CT bronchus sign (%)	69	74	0.31

*Univariate analysis: chi-squared test and *t*-tests were performed for proportional differences or mean differences in variables between training and validation sets (two-sided).

CEA, carcinoembryonic antigen; LLL, left lower lobe; LUL, left upper lobe; RLL, right lower lobe; RML, right middle lobe; RUL, right upper lobe.

and each suggests, but does not guarantee, a diagnosis of benign versus malignant SPN. Spiculation, lobulation and vascular convergence are typically associated with malignancy.[23,24] Calcification, a well-defined margin, cavitation and CT bronchus signs including bronchus involvement show considerable overlap between benign and malignant SPNs.[24–28] The reported frequencies of these radiological findings have varied among studies. In the present study, the prediction model identified calcification, spiculation and CT bronchus sign as being useful for distinguishing benign from malignant SPNs. The validity of the present prediction model is supported by the previous prediction model and the typical radiographic features of malignant versus benign SPNs.

There were no differences in the laboratory or radiological results or in the pattern of care for SPN between the training set and the validation set. However, a limitation of the present study is the potential for selection bias, just as in previous studies. Selection bias has arisen because the model is based on a population with clinically suspicious lesions that required resection. It is unclear how this would affect the performance of the prediction model in a more general population. There were significant differences in two radiological variables (mean diameter and calcification) between the training set and the validation set. The prediction model would also need to be validated in other patient populations outside that of our single institution.

The best clinical management of a patient with an SPN requires evaluation of the probability of malignancy, which determines the most cost-effective diagnosis and treatment strategies. In several decision analyses, the probability of malignancy is divided into four categories: low (<10%), intermediate (10–60%), high (>60 to 90%) and very high (>90%).[29,30] The management pathway should take into consideration patient preference and the potential complications after assessment of the probability of malignancy. CT or CXR follow up is preferred in patients with a low probability of malignancy. When the probability is intermediate, additional testing would be required, including contrast-enhanced CT, fine-needle aspiration, bronchoscopy and PET/CT. Surgery is recommended in patients with a high or very high probability of malignancy. PET/CT has become important in differentiating benign from malignant nodules, and its estimated sensitivity for identifying a malignant process is 96%, and its specificity is 88%.[31] Currently, investigators have made efforts to develop a computer-aided diagnosis system for SPN. The computer-aided diagnosis system has the potential to improve diagnostic accuracy of SPN in future.[32]

Radiological examinations such as CT will detect a large number of SPNs. The physician can use the prediction model for differentiating between benign and malignant SPNs. Even if serum CEA and CRP cannot be measured, the alternative prediction model might assist in the evaluation of the probability of malignancy. The prediction model and particular observation of CT imaging for each patient would assist in determining the optimal management and in identifying the indications for invasive and

expensive procedures, such as surgery. Future studies should evaluate the accuracy of this prediction model in a larger cohort or non-Japanese cohort, and whether the clinical decisions made based on the prediction model actually improve clinical outcomes.

ACKNOWLEDGEMENTS

We thank Shingo Takano, Shun-ichi Watanabe, Kenji Suzuki, Yasuaki Arai, Noriyuki Moriyama and Ryosuke Tsuchiya (National Cancer Center Hospital, Tokyo) for their help in carrying out this study.

REFERENCES

1 Holin SN, Dwork RE, Glaser S, Rickli AE, Stocklen JB. Solitary pulmonary nodules found in a community-wide chest roentgenographic survey. *Am. Tuberc. Pulm. Dis.* 1959; **79**: 427–39.
2 Swensen SJ, Silverstein MD, Edell ES, Trastek VF, Aughenbaugh GL *et al.* Solitary pulmonary nodules: clinical prediction model versus physicians. *Mayo Clin. Proc.* 1999; **74**: 319–29.
3 Midthun DE, Swensen SJ, Jett JR. Approach to the solitary pulmonary nodule. *Mayo Clin. Proc.* 1993; **68**: 378–85.
4 Khouri NF, Meziane MA, Zerhouni EA, Fishman EK, Siegelman SS. The solitary pulmonary nodule: assessment, diagnosis, and management. *Chest* 1987; **91**: 128–33.
5 Swensen SJ, Jett JR, Payne WS, Viggiano RW, Pairolero PC *et al.* An integrated approach to evaluation of the solitary pulmonary nodule. *Mayo Clin. Proc.* 1990; **65**: 173–86.
6 Cummings SR, Lillington GA, Richard RJ. Estimating the probability of malignancy in solitary pulmonary nodules. A Bayesian approach. *Am. Rev. Respir. Dis.* 1986; **134**: 449–52.
7 Gurney JW. Determining the likelihood of malignancy in solitary pulmonary nodules with Bayesian analysis. *Radiology* 1993; **186**: 405–13.
8 Swensen SJ, Silverstein MD, Ilstrup DM, Schleck CD, Edell ES. The probability of malignancy in solitary pulmonary nodules. Application to small radiologically indeterminate nodules. *Arch. Intern. Med.* 1997; **157**: 849–55.
9 Baldwin DR, Birchall JD, Ganatra RH, Pointon KS. Evaluation of the solitary pulmonary nodule: clinical management, role of CT and nuclear medicine. *Imaging* 2004; **16**: 22–36.
10 Bates SE. Clinical application of serum tumor markers. *Ann. Intern. Med.* 1991; **115**: 623–85.
11 Ausitn JH, Muller NL, Friedmen PJ, Hansell DM, Naidich DP *et al.* Glossary of terms for CT of the lungs: recommendations of the Nomenclature Committee of the Fleischner Society. *Radiology* 1996; **200**: 327–31.
12 Seemann MD, Seemann O, Luboldt W, Bonel H, Sittek H *et al.* Differentiation of malignant from benign solitary pulmonary lesions using chest radiography, spiral CT and HRCT. *Lung Cancer* 2000; **29**: 105–24.
13 Trunk G, Gracey GR, Byrd RB. The management and evaluation of the solitary pulmonary nodule. *Chest* 1974; **66**: 236–9.
14 Health and Welfare Statistics Association. Tobacco. *J. Health Welfare Stat.* 1997; **44**: 101–4 (in Japanese).
15 Suzuki K, Nagai K, Yoshida J, Nishimura M, Nishiwaki Y. Predictors of lymph node and intrapulmonary metastasis in clinical stage IA non-small cell lung carcinoma. *Ann. Thorac. Surg.* 2001; **72**: 352–6.
16 Sawabata N, Ohta M, Takeda S, Hirano H, Okumura Y *et al.* Serum carinoembryonic antigen level in surgically resected clinical stage I patients with non-small cell lung cancer. *Ann. Thorac. Surg.* 2002; **74**: 174–9.
17 Alexander JC, Silverman NA, Chretien PB. Effect of age and cigarette smoking on carcinoembryonic antigen levels. *JAMA* 1976; **235**: 1975–9.
18 Castell JV, Gomez-Lechon MJ, David M, Fabra R, Trullenque R *et al.* Acute phase response of human hepatocytes: regulation of acute-phase protein synthesis by interleukin-6. *Hepatology* 1990; **12**: 1179–86.
19 Pepys MB, Hirschfield GM. C-reactive protein: a critical update. *J. Clin. Invest.* 2003; **111**: 1805–12.
20 Katsumata N, Eguchi K, Fukuda M, Yamamoto N, Ohe Y *et al.* Serum levels of cytokines in patients with untreated primary lung cancer. *Clin. Cancer Res.* 1996; **2**: 553–9.
21 Yanagawa H, Sone S, Takahashi Y, Haku T, Yano S *et al.* Serum levels of interleukin 6 in patients with lung cancer. *Br. J. Cancer* 1995; **71**: 1095–8.
22 Alexandrakis MG, Passam FH, Perisinakis K, Ganotakis E, Margantinis G *et al.* Serum proinflammatory cytokines and its relationship to clinical parameters in lung cancer patients with reactive thrombocytosis. *Respir. Med.* 2002; **96**: 553–8.
23 McKeown DJ, Brown DJF, Kelly A, Wallace AM, McMillan DC. The relationship between circulating concentrations of C-reactive protein, inflammatory cytokines and cytokine receptors in patients with non-small-cell lung cancer. *Br. J. Cancer* 2004; **91**: 1993–5.
24 Siegelman SS, Khouri NF, Leo FP, Fishman EK, Braverman RM *et al.* Solitary pulmonary nodules: CT assessment. *Radiology* 1986; **160**: 307–12.
25 Erasmus JJ, Connolly JE, McAdams HP, Roggli VL. Solitary pulmonary nodules: part I. Morphologic evaluation for differentiation of benign and malignant lesions. *Radiographics* 2000; **20**: 43–58.
26 Qiang JW, Zhou KR, Lu G, Wang Q, Ye XG *et al.* The relationship between solitary pulmonary nodules and bronchi: multi-slice CT-pathological correlation. *Clin. Radiol.* 2004; **59**: 1121–7.
27 Grewal RG, Austin JHM. CT demonstration of calcification in carcinoma of the lung. *J. Comput. Assist. Tomogr.* 1994; **18**: 867–71.
28 Takashima S, Sone S, Li F, Maruyama Y, Hasegawa M *et al.* Indeterminate solitary pulmonary nodules revealed at population based CT screening of the lung. *Am. J. Roentgenol.* 2003; **180**: 1255–63.
29 Decamp MM. The solitary pulmonary nodule: aggressive excisional strategy. *Semin. Thorac. Cardiovasc. Surg.* 1992; **14**: 292–6.
30 Gambhir SS, Shepherd JE, Shah BD, Hart E, Hoh CK *et al.* Analytical decision model for the cost effective management of solitary pulmonary nodules. *J. Clin. Oncol.* 1998; **16**: 2113–25.

31 Yi CA, Lee KS, Kim BT, Choi JY, Kwon OJ *et al.* Tissue characterization of solitary pulmonary nodule: comparative study between helical dynamic CT and integrated PET/CT. *J. Nucl. Med.* 2006; **47**: 443–50.

32 Li F, Aoyama M, Shiraishi J, Abe H, Li Q *et al.* Radiologists' performance for differentiating benign from malignant lung nodules on high-resolution CT using computer-estimated likelihood of malignancy. *Am. J. Roentgenol.* 2004; **183**: 1209–15.

Pathology International 2008; **58**: 31–37 doi:10.1111/j.1440-1827.2007.02185.x

Original Article

Immunohistochemical expression of TTF-1 in various cytological subtypes of primary lung adenocarcinoma, with special reference to intratumoral heterogeneity

Akiko M. Maeshima,[1] Mutsuko Omatsu,[1] Koji Tsuta,[1] Hisao Asamura[2] and Yoshihiro Matsuno[1]*

[1]*Clinical Laboratory Division and* [2]*Thoracic Surgery Division, National Cancer Center Hospital, Tokyo, Japan*

The immunohistochemical expression of thyroid transcription factor-1 (TTF-1) was investigated in various cytological subtypes of primary lung adenocarcinoma, with special reference to intratumoral heterogeneity. Three groups were categorized according to cytological subtype: group A, adenocarcinomas with either a Clara cell and/or type II epithelial cell component (Clara/type II) or a mixed Clara/type II and bronchial surface epithelial cell component (BSE) (mCB), in addition to other components; group B, adenocarcinomas with components including either BSE, a goblet cell component (GOB) or a mixed BSE and GOB component (mBG), and lacking Clara/type II or mCB; group C, adenocarcinomas with only a poorly differentiated component (POR). In group A all Clara/type II, mCB, BSE and the majority of POR were TTF-1 positive. In group B the majority of BSE, POR and all GOB were TTF-1 negative. BSE and POR in both groups had a different phenotype, possibly reflecting their different natural history. In group C 80% of cases were TTF-1 positive, suggesting that the majority were derived from group A tumors.

Key words: adenocarcinoma, immunohistochemistry, intratumoral heterogeneity, lung, TTF-1

Thyroid transcription factor (TTF) is a 38 kDa DNA-binding protein containing a homeodomain. It was originally identified in thyroid follicular cells as a regulator of thyroid-specific genes, such as those responsible for the production of thyroglobulin,[1,2] thyroperoxidase,[2,3] and thyrotropin receptor.[4] In addition to thyroid epithelial cells, TTF-1 was subsequently found in epithelial cells of the respiratory tract, and in areas of the developing brain.[5,6] In adult lung, TTF-1 is expressed in type II pneumocytes, non-ciliated bronchiolar epithelial cells (Clara cells) and bronchiolar basal cells,[7] and is responsible for transcriptional activation of surfactant proteins A, B, and C, as well as Clara cell secretory proteins by direct binding to the promoters of these molecules.[8–11]

Neoplasms of pulmonary origin retain expression of TTF-1, although immunoreactivity varies according to histological tumor type. It has been reported that TTF-1 is expressed in 75–80% of adenocarcinomas[12–23] and >90% of small cell carcinomas,[24–26] whereas it is found at very low frequency in squamous cell carcinomas[14–16,20,21] and large cell carcinomas.[13,14,16] Previous reports have indicated that its expression does not seem to be closely related to the histological pattern of adenocarcinoma growth, because it has been found in tumors with acinar, papillary, and bronchioloalveolar morphology.[13,14,16,17,19] However, there is growing evidence that adenocarcinomas with a predominantly mucinous component tend to be TTF-1 negative.[13,27–29] Particularly, mucinous-type bronchioloalveolar carcinomas, in contrast to non-mucinous bronchioloalveolar carcinomas, tend to be uniformly negative.[13,27,28] Yatabe *et al.* reported that adenocarcinomas with terminal respiratory unit (TRU) morphology, resembling type II pneumocytes, Clara cells, and/or bronchioles, were frequently (88%) TTF-1 positive, whereas only 25% of adenocarcinomas without TRU morphology expressed TTF-1.[22] In contrast, it is noteworthy that there is significant morphological variation in lung adenocarcinoma, not only among tumors, but also within a single tumor. Thus, the relationship between cytological characteristics or histological patterns and TTF-1 expression in adenocarcinoma should be studied in more detail.

In the World Health Organization (WHO) classification, adenocarcinomas are subdivided into bronchioloalveolar carcinoma (non-mucinous type and mucinous type), papillary adenocarcinoma, acinar adenocarcinoma and solid

Correspondence: Yoshihiro Matsuno, MD, Clinical Laboratory Division, National Cancer Center Hospital, 5-1-1 Tsukiji, Chuo-ku, Tokyo 104-0045, Japan. Email: ymatsuno@med.hokudai.ac.jp

*Present address: Department of Surgical Pathology, Hokkaido University Hospital, Sapporo, Japan.

Received 16 May 2007. Accepted for publication 2 September 2007.

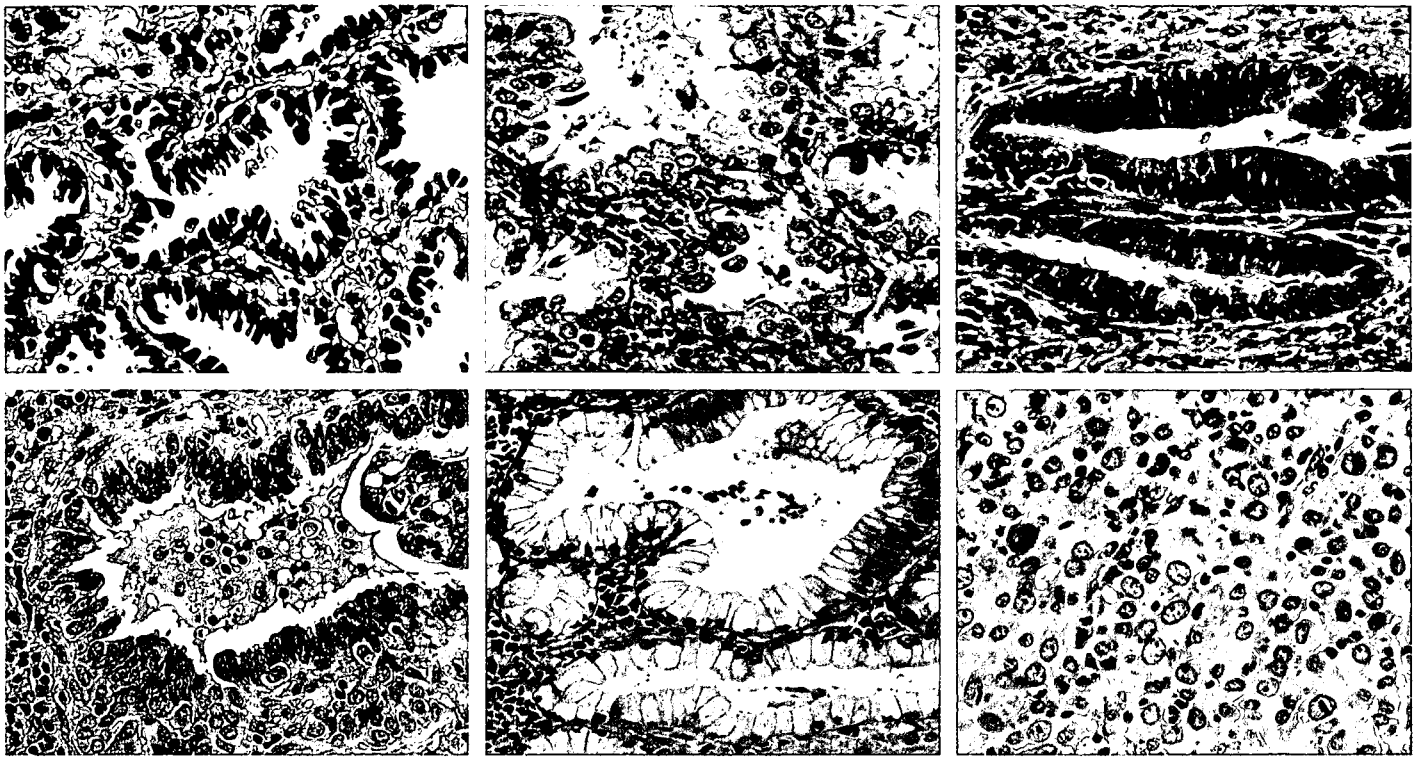

Figure 1 (**a**) Clara; (**b**) Type II; (**c**) bronchial surface epithelial component (BSE); (**d**) mixed Clara/type II and BSE component (mCB); (**e**) goblet cell component (GOB); (**f**) poorly differentiated component (POR) (HE).

adenocarcinoma with mucin, according to structural pattern.[30] For cytological types, Shimosato *et al.* followed the original proposal by Kimula[31] and subclassified adenocarcinoma into six cytological types:[32] Clara cell type, type II alveolar epithelial cell type, bronchial surface cell type with little or no mucus production, goblet cell type, bronchial gland cell type, and mixed cell type or intermediate cell type.

In the present study we subdivided adenocarcinomas into the following cytological components by modifying the cytological classification of Shimosato: Clara cell and/or type II alveolar epithelial component, bronchial surface epithelial component, goblet cell component, poorly differentiated component, and mixed types. We examined in more detail the relationship between various cytological subtypes of adenocarcinomas and TTF-1 expression, with special reference to intratumoral heterogeneity, in order to better understand the carcinogenesis and natural history of pulmonary adenocarcinoma.

MATERIALS AND METHODS

Patients and histological evaluation

A total of 779 patients with primary lung adenocarcinomas, who underwent lobectomy between 1998 and 2002 at the National Cancer Center Hospital, Tokyo, Japan, were analyzed. Resected lung tissues were fixed with 10% formalin for 1 or 2 days, embedded in paraffin and sliced into 4 μm-thick sections. Histological findings in each case were reviewed independently by at least two pulmonary pathologists (AMM, KT, YM).

Tumor cell morphology

Adding some modification to Kimula's and Shimosato's descriptions, cytological components in each adenocarcinoma were subdivided according to the morphological features of routinely prepared HE-stained paraffin sections as follows: Clara cell component and/or type II alveolar epithelial component (Clara/type II), bronchial surface epithelial component (BSE), goblet cell component (GOB), poorly differentiated component (POR) and mixed types. The Clara cell component was defined by the presence of hobnail-shaped or cuboidal cells with eosinophilic cytoplasm, or columnar cells with an apical snout (Fig. 1a). The type II alveolar epithelial component was defined by cuboidal or low-columnar cells with clear or vacuolated cytoplasm (Fig. 1b). Because these two components often appeared admixed, and could not be distinguished from each other, a single category of Clara/type II was established. BSE was

Table 1 Definition of three groups of lung adenocarcinomas

Group A: Adenocarcinomas with either Clara/type II or mCB, in addition to other components
Group B: Adenocarcinomas with components including either BSE, GOB or mBG, and lacking Clara/type II or mCB
Group C: Adenocarcinomas with only POR

BSE, bronchial surface epithelial component; GOB, goblet cell component; mCB, mixed Clara/type II and BSE component; mBG, mixed BSE and GOB component; POR, poorly differentiated component.

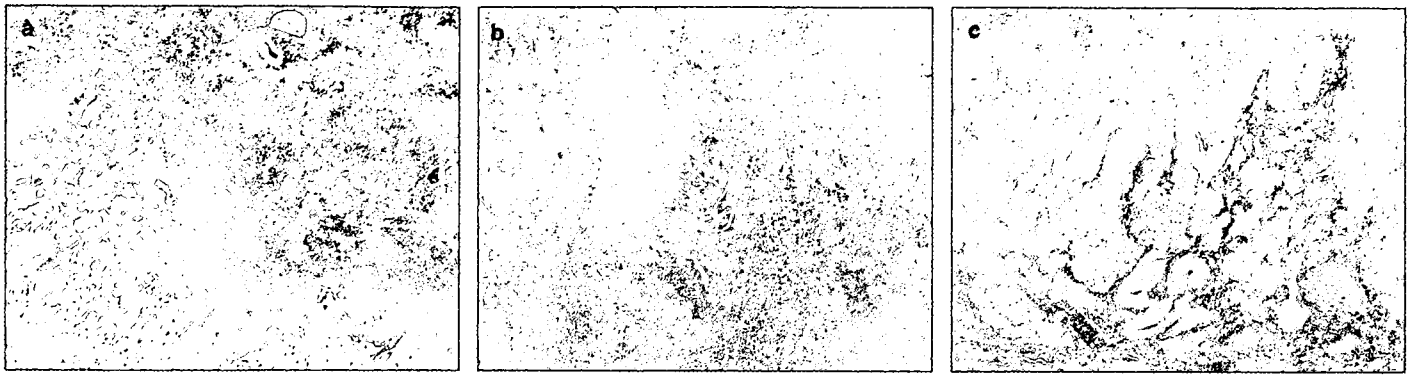

Figure 2 (**a**) Clara (bottom), bronchial surface epithelial component (BSE) (left) and poorly differentiated component (POR) (right) in group A tumor. (**b**) BSE (left), GOB (middle) and POR (right) in group B tumor. (**c**) Group C tumor (HE).

defined by tall columnar cells with eosinophilic cytoplasm and a smooth luminal surface (Fig. 1c). When a tumor contained areas showing an intimate admixture of Clara/type II- and BSE-type cells, and also admixed with columnar cells indeterminate for Clara/type II- or BSE-type cells, it was judged as having a mixed Clara/type II and BSE component (mCB, Fig. 1d). GOB was defined by tall columnar cells with plump mucinous cytoplasm, a smooth surface and a basally displaced nucleus (Fig. 1e). A component showing a close admixture of BSE- and GOB-type cells, and/or showing cells indistinguishable from either BSE- or GOB-type cells, was described as a mixed BSE and GOB component (mBG). A cytological component composed of poorly differentiated polygonal cells with mucin was defined as POR (Fig. 1f). This component usually had a solid or scirrhous growth pattern.

In each tumor the presence of areas containing each component was described regardless of predominance. Although many adenocarcinomas contained an extensive variety of these components, adenocarcinomas were further categorized into three groups according to their similarities or shared components: group A, adenocarcinomas showing various proportions of areas of either Clara/type II or mCB, in addition to other components (representing tumors with Clara/type II morphology); group B, adenocarcinomas with components including either BSE, GOB or mBG, and lacking Clara/type II or mCB (representing differentiated tumors without Clara/type II morphology); group C, adenocarcinomas with only POR (Table 1, Fig. 2).

Immunohistochemistry

Representative tissue sections from each case were used for immunohistochemistry. TTF-1 antigen was retrieved by autoclave treatment (121°C, 10 min) with pH 6.0 citrate buffer. The standard avidin–biotin–peroxidase complex method was used for immunohistochemical detection after incubation with a monoclonal antibody against TTF-1 (8G7G3/1, NeoMarkers, Fremont, CA, USA). Immunostaining was performed within 1 week of preparation of the tissue slides. Positive nuclear staining of non-neoplastic type II pneumocytes served as an internal control for antigen preservation. The extent of tumor cells with positive nuclear staining was graded using five categories: 0, 0% (negative); 1+, 1–10%; 2+, 11–50%; 3+, 51–90%; 4+, 91–100%.

RESULTS

According to the categorization, the 779 cases analyzed comprised 689 group A adenocarcinomas, 80 group B adenocarcinomas and 10 group C adenocarcinomas. Among them, a sequential series of 147 cases consisting of 104 group A, 33 group B and 10 group C were used for further study. According to the WHO tumor classification,[30] 101 of the tumors were diagnosed as adenocarcinomas of mixed subtypes, 31 as bronchioloalveolar carcinomas, 10 as solid adenocarcinomas with mucin, and five as acinar adenocar-

Table 2 Extent of immunohistochemical TTF-1 expression in adenocarcinomas of the lung

Positive degree	0 (0%: negative)	1+ (1–10%)	2+ (11–50%)	3+ (51–90%)	4+ (91–100%)
Group A, 104 tumors	0	1 (1%)	10 (10%)	29 (27%)	65 (62%)
Components					
Clara/type II ($n = 87$)	0	1	5	4	77
mCB ($n = 39$)	0	1	7	9	22
BSE ($n = 5$)	0	1	2	1	1
GOB ($n = 1$)	1	0	0	0	0
POR ($n = 44$)	3	6	9	14	12
Group B, 33 tumors	26 (79%)	4 (12%)	2 (6%)	0	1 (3%)
Components					
BSE ($n = 15$)	9	3	2	0	1
mBG ($n = 10$)	9	1	0	0	0
GOB ($n = 8$)	8	0	0	0	0
POR ($n = 15$)	11	2	1	0	1
Group C, 10 tumors	2 (20%)	1 (10%)	2 (20%)	3 (30%)	2 (20%)
POR ($n = 10$)	2	1	2	3	2

BSE, bronchial surface epithelial component; GOB, goblet cell component; mCB, mixed Clara/type II and BSE component; mBG, mixed BSE and GOB; POR, poorly differentiated component; TTF-1, thyroid transcription factor-1.

cinomas. The patients consisted of 80 men and 67 women, ranging in age from 26 to 81 years with a mean age of 62 years. Maximum tumor diameter ranged from 0.7 cm to 13.0 cm with a mean diameter of 3.1 cm.

In group A 104 tumors (100%) contained areas with Clara/type II or mCB as a component by definition. Among them, 87 (84%) had Clara/type II, 39 (38%) had mCB. As for other components identified in tumors in this group, five (4%) had BSE, one (1%) had GOB and 44 (42%) had POR. In group B, 15 (45%) had BSE, 10 (30%) had mBG, eight (24%) had GOB and 15 (45%) had POR, as cytological components. Group C consisted of only POR by definition.

The extent of TTF-1 immunohistochemical staining of tumor cell nuclei is summarized in Table 2, and examples of staining patterns are shown in Fig. 3. Immunostaining extent and intensity were usually parallel. Tumors with 3+ or 4+ TTF-1 staining mostly had a strong staining pattern. A total of 81% (119/147 tumors) of all adenocarcinomas were positive for TTF-1 in at least a few percent of the tumor cells.

In group A all the tumors were TTF-1 positive. Specifically, all of the Clara/type II, mCB and BSE components were TTF-1 positive, showing strong immunoreactivity in most cases. A proportion of group A tumors with marked nuclear atypia showed a low extent and weak intensity of TTF-1 expression. GOB, found in only one case in group A, was TTF-1 negative; 93% (41/44 lesions) of POR were TTF-1 positive. Thus, most of the group A tumors had TTF-1 expression even in BSE or POR.

In group B 21% (7/33) of tumors were TTF-1 positive. Specifically, 40% (6/15 lesions) of BSE, 10% (1/10 lesions) of mBG, 0% (0/8 lesions) of GOB and 27% (4/15 lesions) of POR were TTF-1 positive. In group C 80% (8/10) of tumors were TTF-1 positive.

Table 3 highlights the difference of TTF-1 positivity among the same morphological components BSE and POR found in different groups. Although they are categorized as an identical cytomorphological component, TTF-1 expression was more frequent in components found in group A tumors.

DISCUSSION

We examined the immunohistochemical expression of TTF-1 in various cytological subtypes of primary lung adenocarcinoma, with special reference to intratumoral heterogeneity, in order to better understand the natural history of lung adenocarcinoma.

In group A all Clara/type II and mCB were TTF-1 positive. Moreover, TTF-1 expression was maintained in all BSE and the majority of POR. These findings suggest two important facts. First, in lung adenocarcinomas with a hobnail or cuboidal morphology, TTF-1 will always be positive if a lung adenocarcinoma is primary. If TTF-1 is negative, then metastatic adenocarcinoma should be considered by priority even if the morphology is similar. Second, the natural history of group A tumors, suggested on the basis of morphology, is that they are derived from peripheral alveolar epithelium, and acquire heterogeneity and undergo dedifferentiation during progression according to cytological and structural morphology, which is consistent with retention of TTF-1 expression through Clara/type II, mCB, BSE and POR. The latter hypothesis is compatible with the description of Yatabe *et al.*,[22] that is, adenocarcinomas with TRU morphology, resembling type II pneumocytes, Clara cells, and/or bronchioles, were frequently (88%) TTF-1 positive, and TTF-1-positive adenocarcinomas frequently maintained TTF-1 immunoreactivity at

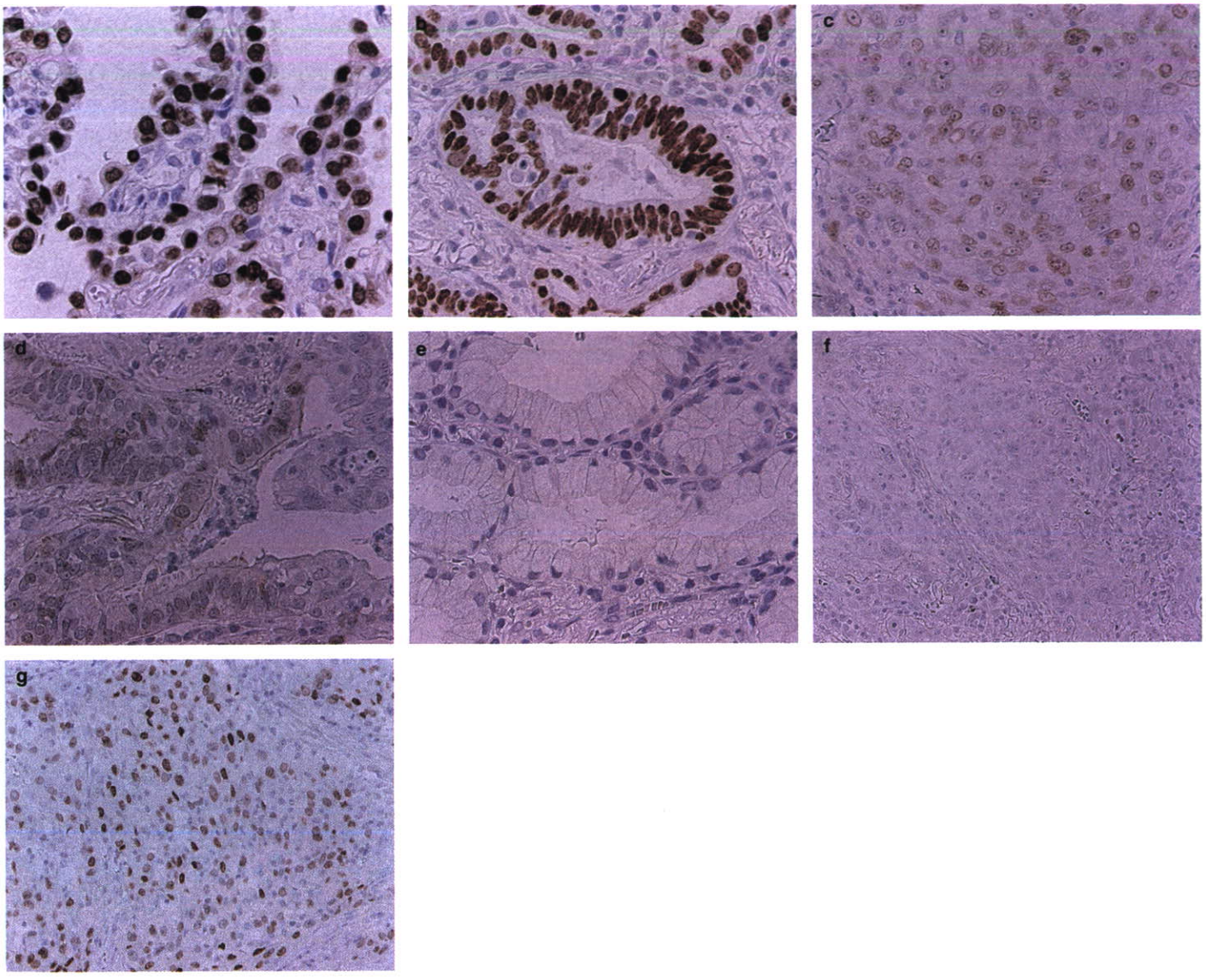

Figure 3 Immunohistochemical thyroid transcription factor-1 expression. Strongly positive in (**a**) Clara and (**b**) bronchial surface epithelial component (BSE), and weakly positive in (**c**) poorly differentiated component (POR) in group A tumor. Weakly positive in (**d**) BSE, and negative in (**e**) GOB and (**f**) POR in group B tumor. (**g**) Positive in group C tumor. (HE).

Table 3 Immunohistochemical TTF-1 expression in adenocarcinomas

Positive degree	0 (0%: negative)	1+ (1–10%)	2+ (11–50%)	3+ (51–90%)	4+ (91–100%)
BSE (no. cases)					
Group A ($n = 5$)	0	1	2	1	1
Group B ($n = 15$)	9	3	2	0	1
POR					
Group A ($n = 44$)	3	6	9	14	12
Group B ($n = 15$)	11	2	1	0	1
Group C ($n = 10$)	2	1	2	3	2

BSE, bronchial surface epithelial component; POR, poorly differentiated component; TTF-1, thyroid transcription factor-1.

metastatic sites even if they had dedifferentiated to poorly differentiated adenocarcinoma.

BSE in group B (lacking Clara/type II or mCB) were frequently TTF-1 negative, in contrast to constant TTF-1 expression of BSE in group A. Although it is impossible to distinguish a BSE component of these two groups solely on the basis of cytological and structural morphology, the natural histories through which they acquire their morphologies may

be different. Group B tumors are suspected to be derived from bronchial epithelium or bronchial metaplastic epithelium, and not from peripheral alveolar epithelium such as group A tumors. Although the possibility remains that group B tumors are derived from peripheral alveolar epithelium and lose their TTF-1 expression completely during progression, this seems unlikely when considering the difference in cytological constituents between these two groups, as well as the conserved expression of TTF-1 in group A. A similar hypothesis can be suggested for POR. Although POR in group A and POR in group B show similar morphology, they are suggested to have different characters (history and biological nature), which reflect the presumed natural history of each group.

All GOB lesions were TTF-1 negative, both in group A and in group B. Although most goblet cell adenocarcinomas are of the pure form, small numbers of mixed goblet cell and non-goblet cell adenocarcinoma also exist.[27,33] Lau *et al.* reviewed seven cases of mixed non-mucinous and mucinous BAC, and reported that 6/7 of the mucinous component (almost identical to BAC comprising only the goblet component) were TTF-1 negative, whereas 5/7 of the non-mucinous component were TTF-1 positive.[27] Also in the present study, the non-goblet cell component in mixed goblet cell and non-goblet cell adenocarcinomas in both groups A and B expressed TTF-1 in some cases. On the basis of previous reports and the present data, we hypothesize that TTF-1 expression is completely lost when adenocarcinomas differentiate to a goblet cell morphology in mixed goblet cell and non-goblet cell adenocarcinoma. However, in pure goblet cell adenocarcinoma it is difficult to explain the lack of TTF-1 expression, and therefore the mechanism of controlling TTF-1 expression should be clarified from the viewpoint of the physiological function of TTF-1 and mucin production.

Eight of 10 group C tumors were TTF-1 positive and some of them expressed TTF-1 strongly. Although their number was small, it is suggested that the majority of group C tumors were derived from group A tumors.

In summary, group A and group B tumors are suggested to have different natural histories, from the viewpoint of immunohistochemical expression of TTF-1. Group A tumors might be derived from peripheral alveolar epithelial cells and retain their TTF-1 expression even if they differentiate to BSE or dedifferentiate to POR. Conversely, the majority of BSE and POR in group B tumors were TTF-1 negative. Although BSE and POR in both groups had a similar morphology, their TTF-1 expression patterns were different, thus reflecting their different natural histories. From the viewpoint of TTF-1 expression, the majority of group C tumors are suggested to be derived from group A tumors.

ACKNOWLEDGMENTS

This work was supported in part by Grant-in-aid for Cancer Research from the Ministry of Health, Labor and Welfare of Japan. The authors are grateful to Ms S. Miura and C. Kina for their excellent technical assistance.

REFERENCES

1 Civitareale D, Lonigro R, Sinclair AJ, Di Lauro R. A thyroid-specific nuclear protein essential for tissue-specific expression of the thyroglobulin promoter. *EMBO J* 1989; **8**: 2537–43.
2 Guazzi S, Price M, De Felice M, Damante G, Mattei MG, Di Lauro R. Thyroid nuclear factor 1 (TTF-1) contains a homeodomain and displays a novel DNA binding specificity. *EMBO J* 1990; **9**: 3631–9.
3 Mizuno K, Gonzalez FJ, Kimura S. Thyroid-specific enhanced-binding protein (T/EBP): cDNA cloning, functional characterization, and structural identity with thyroid transcription factor 1 (TTF-1). *Mol Cell Biol* 1991; **11**: 4927–33.
4 Civitareale D, Castelli MP, Falasca P, Saiardi A. Thyroid transcription factor 1 activates the promoter of the thyrotropin receptor gene. *Mol Endocrinol* 1993; **7**: 1589–95.
5 Lazzaro D, Price M, de Felice M, Di Lauro R. The transcription factor TTF-1 is expressed at the onset of thyroid and lung morphogenesis and in restricted regions of the fetal brain. *Development* 1991; **113**: 1093–104.
6 Kimura S, Hara Y, Pineau T *et al.* The T/ebp null mouse: Thyroid-specific enhancer binding protein is essential for the organogenesis of the thyroid, lung, ventral forebrain, and pituitary. *Genes Dev* 1996; **10**: 60–69.
7 Nakamura N, Miyagi E, Murata S, Kawaoi A, Katoh R. Expression of thyroid transcription factor-1 in normal and neoplastic lung tissues. *Mod Pathol* 2002; **15**: 1058–67.
8 Bruno MD, Bohinski RJ, Huelsman KM, Whitsett JA, Korfhagen TR. Lung cell-specific expression of the murine surfactant protein A (SP-A) gene is mediated by interactions between the SP-A promoter and thyroid transcription factor-1. *J Biol Chem* 1995; **270**: 6531–6.
9 Bohinski RJ, Di Lauro R, Whitsett J. The lung-specific surfactant protein B gene promoter is a target for thyroid transcription factor 1 and hepatocyte nuclear factor 3, indicating common factors for organ-specific gene expression along the foregut axis. *Mol Cell Biol* 1994; **14**: 5671–81.
10 Kelly SE, Bachurski CJ, Burhans MS, Glasser SW. Transcription of the lung-specific surfactant protein C gene is mediated by thyroid transcription factor 1. *J Biol Chem* 1996; **271**: 6881–8.
11 Zhang L, Whitsett JA, Strip BR. Regulation of Clara cell secretory protein gene transcription by thyroid transcription factor-1. *Biochim Biophys Acta* 1997; **1350**: 359–67.
12 Holzinger A, Dingle S, Bejarano PA *et al.* Monoclonal antibody to thyroid transcription factor-1: Production, characterization, and usefulness in tumor diagnosis. *Hybridoma* 1996; **15**: 49–53.
13 Kaufmann O, Dietel M. Thyroid transcription factor-1 is the superior immunohistochemical marker for pulmonary adenocarcinomas and large cell carcinomas compared with surfactant proteins A and B. *Histopathology* 2000; **36**: 8–16.
14 Fabbro D, di Loreto C, Stamerra O, Beltrami CA, Lonigro R, Damante G. TTF-1 gene expression in human lung tumors. *Eur J Cancer* 1996; **32A**: 512–17.

15 Di Loreto C, Di Lauro V, Puglisi F, Damante G, Fabbro D, Beltrami CA. Immunocytochemical expression of tissue specific transcription factor-1 in lung carcinoma. *J Clin Pathol* 1997; **50**: 30–32.
16 Khoor A, Whitsett JA, Stahlman MT, Olson SJ, Cagle PT. Utility of surfactant protein B precursor and thyroid transcription factor 1 in differentiating adenocarcinoma of the lung from malignant mesothelioma. *Hum Pathol* 1999; **30**: 695–700.
17 Bejarano PA, Baughman RP, Biddinger PW *et al.* Surfactant proteins and thyroid transcription factor-1 in pulmonary and breast carcinomas. *Mod Pathol* 1996; **9**: 445–52.
18 Bohinski RJ, Bejarano PA, Balko G, Warnick RE, Whitsett JA. Determination of lung as the primary site of cerebral metastatic adenocarcinomas using monoclonal antibody to thyroid transcription factor-1. *J Neurooncol* 1998; **40**: 227–31.
19 Di Loreto C, Puglisi F, Di Lauro V, Damante G, Beltrami CA. TTF-1 protein expression in pleural malignant mesotheliomas and adenocarcinomas of the lung. *Cancer Lett* 1998; **124**: 73–8.
20 Harlamert HA, Mira J, Bejarano PA *et al.* Thyroid transcription factor-1 and cytokeratin 7 and 20 in pulmonary and breast carcinoma. *Acta Cytol* 1998; **42**: 1382–8.
21 Pelosi G, Fraggetta F, Pasini F *et al.* Immunoreactivity for thyroid transcription factor-1 in stage I non-small cell carcinomas of the lung. *Am J Surg Pathol* 2001; **25**: 363–72.
22 Yatabe Y, Mitsudomi T, Takahashi T. TTF-1 expression in pulmonary adenocarcinomas. *Am J Surg Pathol* 2002; **26**: 767–73.
23 Stenhouse G, Fyfe N, King G, Chapman A, Kerr KM. Thyroid transcription factor 1 in pulmonary adenocarcinoma. *J Clin Pathol* 2004; **57**: 383–7.
24 Folpe AL, Gown AM, Lamps LW *et al.* Thyroid transcription factor-1: Immunohistochemical evaluation in pulmonary neuroendocrine tumors. *Mod Pathol* 1999; **12**: 5–8.
25 Byrd-Gloster AI, Khoor A, Glass LF *et al.* Differential expression of thyroid transcription factor 1 in small cell lung carcinoma and Merkel cell tumor. *Hum Pathol* 2000; **31**: 59–62.
26 Ordonez NG. Value of thyroid transcription factor-1 immunostaining in distinguishing small cell lung carcinoma from other small cell carcinomas. *Am J Surg Pathol* 2000; **24**: 1217–23.
27 Lau SK, Desrochers M, Luhringer DJ. Expression of thyroid transcription factor-1, cytokeratin 7, and cytokeratin 20 in bronchioloalveolar carcinomas: An immunohistochemical evaluation of 67 cases. *Mod Pathol* 2002; **15**: 538–42.
28 Copin MC, Buisine MP, Leteurtre E *et al.* Mucinous bronchioloalveolar carcinomas display a specific pattern of mucin gene expression among primary lung adenocarcinomas. *Hum Pathol* 2001; **32**: 274–81.
29 Goldstein NS, Thomas M. Mucinous and nonmucinous bronchioloalveolar adenocarcinomas have distinct staining patterns with thyroid transcription factor and cytokeratin 20 antibody. *Am J Clin Pathol* 2001; **116**: 319–25.
30 Travis WD, Colby TV, Corrin B, Shimosato Y, Brambilla E, eds. *World Health Organization International Histological Classification of Tumours, Histological Typing of Lung and Pleural Tumours*, 3rd edn. Berlin: Springer, 2002.
31 Kimula Y. A histochemical and ultrastructural study of adenocarcinoma of the lung. *Am J Surg Pathol* 1978; **2**: 253–64.
32 Shimosato Y, Noguchi M. Pulmonary neoplasms. In: Mills SE, ed. *Sternberg's Diagnostic Surgical Pathology*, 4th edn. Philadelphia, PA: Lippincott Williams & Wilkins, 2004; 1173–222.
33 Maeshima A, Sakamoto M, Hirohashi S. Mixed mucinous-type and non-mucinous-type adenocarcinoma of the lung: Immunohistochemical examination and K-ras gene mutation. *Virchows Arch* 2002; **440**: 598–603.

Analysis of Expression Patterns of Breast Cancer–Specific Markers (Mammaglobin and Gross Cystic Disease Fluid Protein 15) in Lung and Pleural Tumors

Yuji Takeda, MD; Koji Tsuta, MD; Yasuo Shibuki, CT; Tatsuhiro Hoshino, MD; Naobumi Tochigi, MD; Akiko Miyagi Maeshima, MD; Hisao Asamura, MD; Yuko Sasajima, MD; Tsuyoshi Ito, MD; Yoshihiro Matsuno, MD

• ***Context.***—**The lung is the most common site of metastasis during the natural history of malignant tumors. Breast carcinoma has a propensity for distant metastasis, and the lung and pleura are among the most common metastatic sites. Although it is often difficult to make a clear-cut differential diagnosis between the two, distinguishing primary lung carcinoma from breast carcinoma metastatic to the lung is important because the treatment modalities are different.**

Objective.—**To elucidate the utility of mammaglobin and gross cystic disease fluid protein 15 (GCDFP-15), which are known to be breast-specific antigens, in distinguishing various primary lung and pleural tumors from breast carcinoma metastasizing to the lung.**

Design.—**A total of 20 cases of breast carcinoma metastatic to the lung and 263 tumors of nonbreast origin located in the lung and pleura were analyzed.**

Results.—**Of the 20 cases of breast carcinoma metastatic to the lung, 10 (50.0%) were immunoreactive for mammaglobin and 9 (45.0%) for GCDFP-15, the frequency of positivity being slightly higher for the former than for the latter. The area immunopositive for mammaglobin showed more diffuse staining than the area immunopositive for GCDFP-15. Furthermore, the specificity of mammaglobin for breast carcinoma metastatic to the lung was superior (98.9%) to that of GCDFP-15 (91.8%).**

Conclusion.—**The sensitivity of mammaglobin is equal or superior to that of GCDFP-15 for investigation of breast carcinoma. Immunopositivity for mammaglobin is more diffuse than that for GCDFP-15. In terms of practical diagnosis, mammaglobin immunohistochemistry can serve as a differential marker of breast carcinoma and should be added to the immunohistochemical panel.**

(***Arch Pathol Lab Med.*** **2008;132:239–243)**

The lung is the most common site of metastasis during the natural history of malignant tumors.[1] In particular, breast carcinoma has a propensity for distant metastasis, and the lung and pleura are the second most common metastatic sites following bone.[2] It is also well known that breast carcinoma metastatic to the lung may be found even after a postoperative disease-free interval up to 20 years after resection of the primary lesion. Distinction of primary lung carcinoma from breast carcinoma metastatic to the lung is important under certain clinical situations, such as when a solitary solid nodule is found in the peripheral lung of a patient with a history of resected breast carcinoma, because the treatment modalities for these 2 lesions are different. Furthermore, histologic information regarding hormone receptor status and HER2 status provides a target for therapy in breast carcinoma.

Differentiating between primary lung carcinoma and breast carcinoma metastatic to the lung is often problematic when only a small amount of material is available, as the histologic features may not be sufficient to permit unequivocal distinction. Therefore, reliable immunohistochemical markers are required to facilitate the differentiation of these malignancies.

In breast cancer, the estrogen receptor (ER)/progesterone receptor (PgR) status of the tumor is useful for both prognosis and therapy, with more chemotherapeutic options being available for patients with hormone receptor–positive tumors.[3,4] Breast adenocarcinoma has been shown to be positive for ER in 24% to 63% of cases and positive for PgR in 9% to 37% of cases.[5,6] Breast adenocarcinoma may demonstrate immunophenotypic variability in its expression of ER and PgR, with differences that are dependent on the histologic grade, histologic subtype, antibody clone applied, and immunohistochemical techniques used. These factors limit the sensitivity of these markers for excluding metastatic breast adenocarcinoma in cases of unknown primary site.

When primary unknown metastatic tumor is suspected

Accepted for publication October 12, 2007.

From the Departments of Clinical Laboratory (Drs Takeda, Tsuta, Hoshino, Maeshima, Sasajima, and Matsuno, and Mr Shibuki) and Thoracic Surgery (Drs Hoshino and Asamura), National Cancer Center Hospital, Tokyo, Japan; the Pathology Division, National Cancer Center Research Institute, Tokyo, Japan (Dr Tochigi); and the Department of Thoracic Surgery, Saga University, Saga, Japan (Drs Takeda and Ito).

The authors have no relevant financial interet in the products or companies described in this article.

Reprints: Yoshihiro Matsuno, Clinical Laboratory Division, National Cancer Center Hospital, 1-1 Tsukiji 5-chome, Chuo-ku, Tokyo 104-0045, Japan (e-mail: ymatsuno@med.hokudai.ac.jp).

Table 1. Immunoreactivity of Mammaglobin

	No. of Cases Examined	% Positive	Staining Area			
			0	1+	2+	3+
Breast carcinoma, metastasis to lung	20	50	10	4	6	0
Primary lung carcinoma	250	1.2	247	3	0	0
Adenocarcinoma	100	0	100	0	0	0
Squamous cell carcinoma	60	1.6	59	1	0	0
Pleomorphic carcinoma	20	0	20	0	0	0
Carcinoid tumor	19	5.2	18	1	0	0
Large-cell neuroendocrine carcinoma	20	0	20	0	0	0
Small-cell carcinoma	15	0	15	0	0	0
Adenoid cystic carcinoma	11	9.1	10	1	0	0
Mucoepidermoid carcinoma	5	0	5	0	0	0
Malignant mesothelioma	13	0	20	0	0	0

to have originated from the breast, ER, PgR, and gross cystic disease fluid protein 15 (GCDFP-15) have been shown to be useful immunohistochemical markers.[7-9] However, ER and PgR have also been documented in many neoplasms from various organs. In lung tumors, ER and PgR expressions are reported to range from 0% to 96.7% and from 0% to 46.5%, respectively.[10-12] A panel consisting of anticytokeratin 7 and anticytokeratin 20 (CK7/CK20) antibodies is useful for determining the origin of an unknown primary tumor. However, numerous tumors exhibit an identical $CK7^+/CK20^-$ immunophenotype, including nearly all breast carcinomas and adenocarcinomas of the ovary, lung, endometrial, thyroid, and salivary gland.[13]

Additionally, GCDFP-15 has also been documented in many neoplasms from various locations. In lung tumors, GCDFP-15 expression has been reported to range from 0% to 3.3%[14,15]

The mammaglobin gene sequence fragments were first isolated in 1994 by Watson and Fleming.[16] The mammaglobin gene encodes a 10-kDa molecule, which is related to a family of secretory proteins, including rat prostatic steroid-binding protein subunit C3, human Clara cell 10-kDa protein, and rabbit uteroglobin. Mammaglobin is expressed specifically in breast tissue.[16-18] Recently, an anti-mammaglobin antibody that can be applied to formalin-fixed, paraffin-embedded sections has become commercially available.

In the present study, we elucidated the expression of mammaglobin and GCDFP-15 in order to distinguish various primary lung and pleural tumors from breast carcinoma metastatic to the lung.

MATERIALS AND METHODS

Histologic Analysis

Materials for the present study were extracted from the pathology files of the National Cancer Center Hospital (Tokyo, Japan). The specimens comprised 20 cases of breast carcinoma metastatic to the lung and 263 lung and pleural tumors other than metastatic breast carcinomas: 100 adenocarcinomas, 60 squamous cell carcinomas, 20 pleomorphic carcinomas, 20 large-cell neuroendocrine carcinomas, 15 small-cell carcinomas, 19 carcinoids (14 cases typical and 5 cases atypical), 16 salivary gland–type tumors of the bronchus and/or trachea (11 cases of adenoid cystic carcinoma and 5 cases of mucoepidermoid carcinoma), and 13 malignant pleural mesotheliomas.

The 100 cases of adenocarcinoma were divided into 2 subtypes according to the growth pattern: 60 cases showing lepidic growth and 40 cases without lepidic growth. The 60 cases showing lepidic growth were further divided into 20 cases of the nonmucinous type (tumor cells resembling Clara cells or type II pneumocytes) and 40 cases of the mucinous type (tumor cells resembling goblet cells and/or bronchial surface epithelial cells). Furthermore, the 40 cases without lepidic growth were divided into 20 cases of the acinar-cribriform type (tumor showing an acinar and/or cribriform growth pattern with some degree of cytoplasmic mucin) and 20 cases of the solid type (tumor showing solid growth with some degree of cytoplasmic mucin formation, such as intracytoplasmic lumina).

The 60 cases of squamous cell carcinoma were divided into the well-differentiated type (tumor cells showing a stratified pattern and abundant keratinization), moderately differentiated type (cells showing a lower degree of stratification than that of the well-differentiated type), and poorly differentiated type (the tumor composed of more atypical cells that show only focal squamous cell differentiation).

Immunohistochemistry

For immunohistochemical staining of mammaglobin (clone 304-1A5, 1:200; DAKO, Carpinteria, Calif) and GCDFP-15 (clone D6, 1:200; Signet, Dedham, Mass), 5-μm-thick formalin-fixed sections from each paraffin block were routinely deparaffinized. The sections were exposed to 3% hydrogen peroxide for 15 minutes to block endogenous peroxidase activity, and then washed in deionized water for 2 to 3 minutes. Then, for heat-induced epitope retrieval, the sections stained for mammaglobin were subjected to a 0.02M concentration of citrate buffer (pH 6.0) in a steamer at 120°C for 20 minutes. The sections were allowed to cool at room temperature for 40 minutes, and after rinsing with deionized water and washing in phosphate-buffered saline for 5 minutes, the slides were incubated with primary antibody for 1 hour at room temperature. Then the slides were washed in phosphate-buffered saline 3 times for 5 minutes each time. Subsequently, the slides were labeled with EnVision+/HRP system (DAKO). Diaminobenzidine was used as the chromogen, and Meyer hematoxylin as the counterstain.

Grading the intensity of immunostaining was performed using a sliding scale of 0 to 3+ according to the percentage of reactive cells (0 = <1%; 1+ = 1%–10%; 2+ = 26%–50%; 3+ = 51%–100%).

RESULTS

The results of the immunostains of mammaglobin and GCDFP-15 on each tumor are listed in Tables 1 and 2, respectively.

Breast Carcinoma Metastatic to the Lung

Of the 20 cases of breast carcinoma metastatic to the lung, mammaglobin (Figure 1, A and B) and GCDFP-15 (Figure 1, C and D) stained 10 cases (50.0%) and 9 cases (45.0%), respectively, with mammaglobin showing a

Table 2. Immunoreactivity of Gross Cystic Disease Fluid Protein 15						
	No. of Cases Examined	% Positive	Staining Area			
			0	1+	2+	3+
Breast carcinoma, metastasis to lung	20	45	11	5	4	0
Primary lung carcinoma	250	8.2	231	19		
Adenocarcinoma	100	15	85	15	0	0
Squamous cell carcinoma	60	0	60	0	0	0
Pleomorphic carcinoma	20	5	19	1	0	0
Carcinoid tumor	19	5.2	18	1	0	0
Large-cell neuroendocrine carcinoma	20	0	20	0	0	0
Small-cell carcinoma	15	0	15	0	0	0
Adenoid cystic carcinoma	11	0	11	0	0	0
Mucoepidermoid carcinoma	5	40	3	2	0	0
Malignant mesothelioma	13	0	13	0	0	0

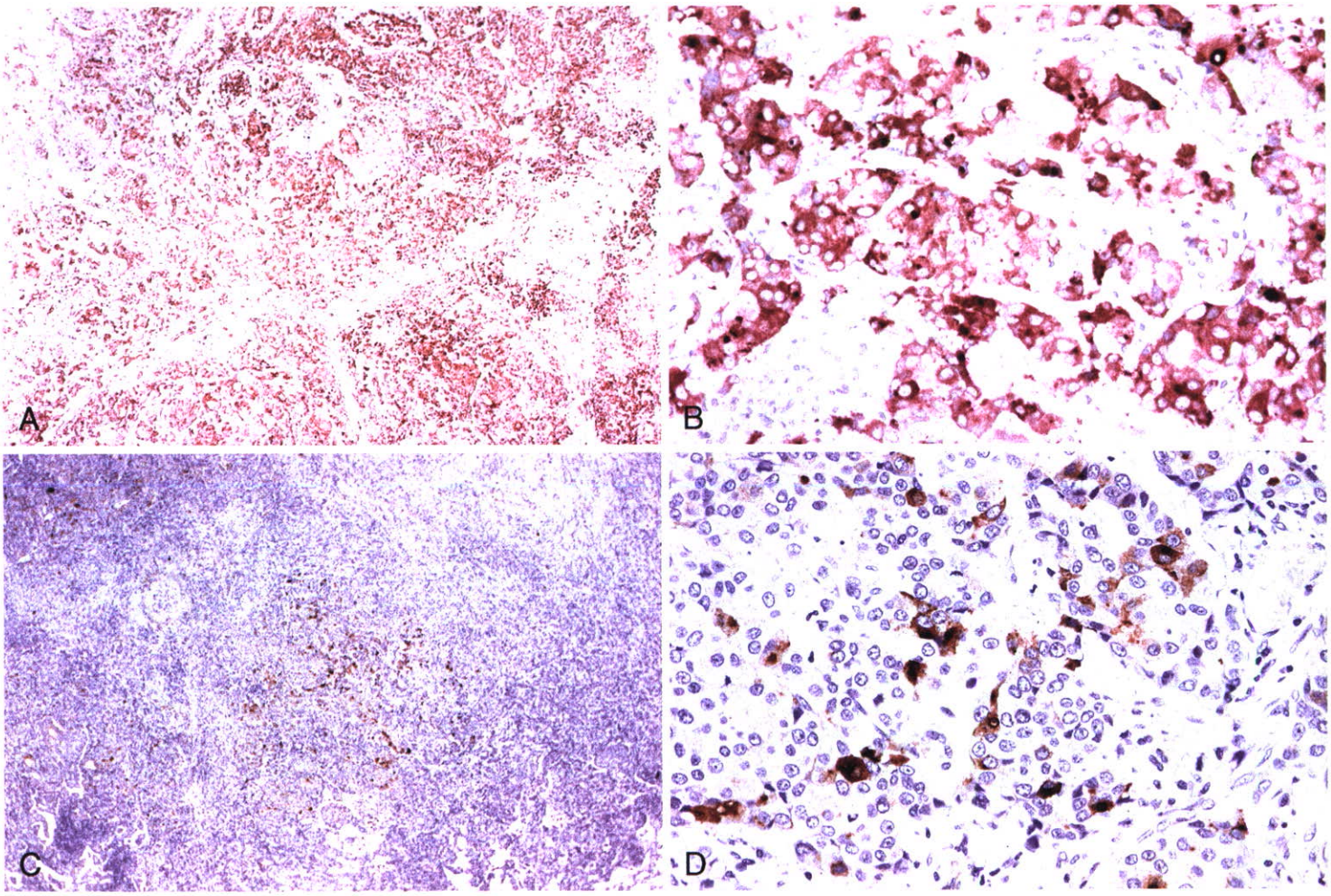

Figure 1. *Breast carcinoma metastatic to the lung, demonstrating solid growth. A to D represent the same case. A and B, Diffuse and strong staining for mammaglobin (original magnifications ×2 [A] and ×20 [B]). C and D, Focal but strong staining for gross cystic disease fluid protein 15 (original magnifications ×2 [C] and ×20 [D]).*

slightly higher frequency of immunostaining than GCDFP-15. Furthermore, mammaglobin showed diffuse immunoreactivity in 60% of immunopositive cases, whereas diffuse immunoreactivity of GCDFP-15 was observed in 44% of all immunopositive cases of breast carcinoma metastatic to the lung. As positivity for either marker was identified in 13 cases, a combination of mammaglobin and GCDFP-15 as a panel raised the sensitivity for identifying breast carcinoma metastatic to the lung to 65%.

The specificity of mammaglobin for detecting breast carcinoma metastatic to the lung (3/263 cases; 98.9%) was higher than that of GCDFP-15 (19/263 cases; 92.8%).

Primary Lung and Pleural Tumors

Primary Lung Adenocarcinomas.—All primary lung adenocarcinomas were immunonegative for mammaglobin. However, GCDFP-15 expression was observed in 15 (15%) of 100 cases of primary lung adenocarcinoma. The lepidic growth pattern was positive in 12 (20%) of 60 cases, and the nonlepidic growth type was positive in 3 (7.5%) of 40 cases. In the lepidic growth type, the non-

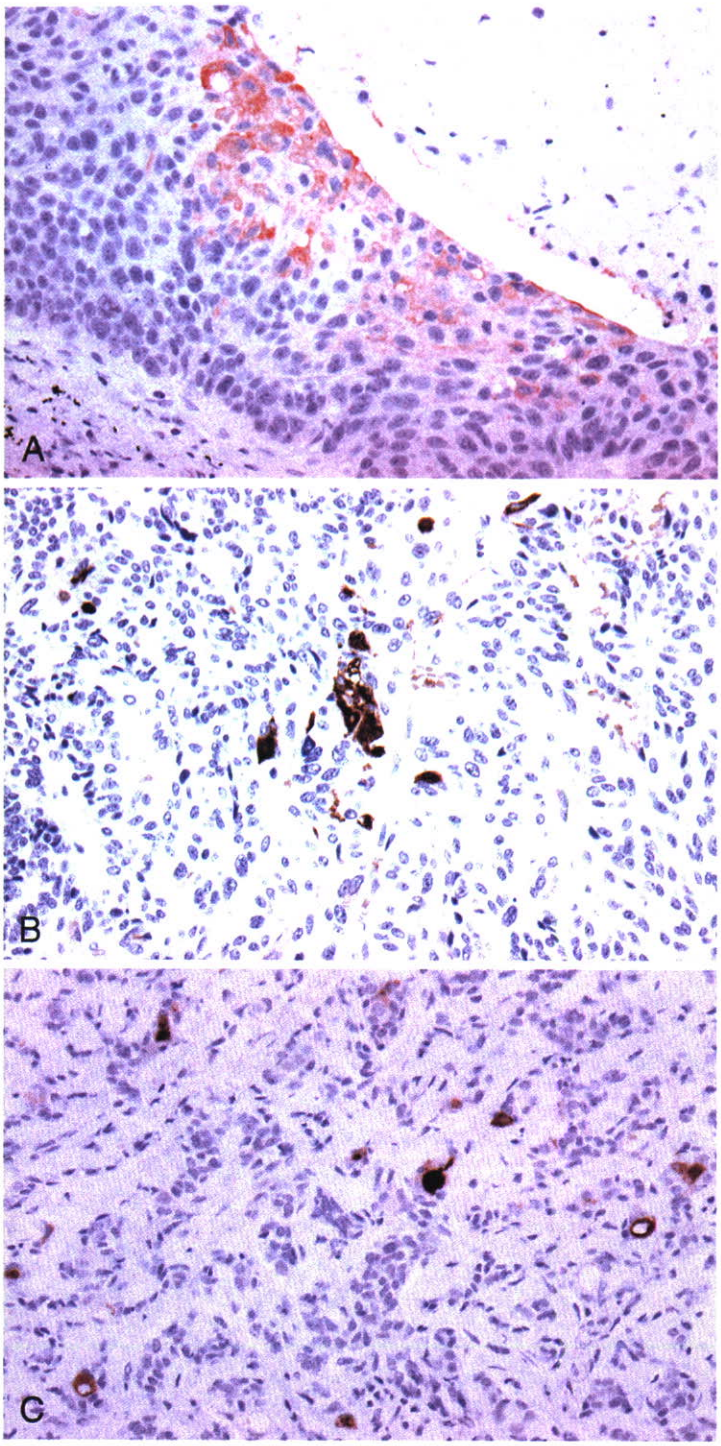

Figure 2. *A, Focal but strong staining for mammaglobin was evident in moderately differentiated squamous cell carcinoma of the lung (original magnification ×20). B, Focal but strong staining for mammaglobin was evident in carcinoid of the lung (original magnification ×20). C, Focal but strong staining for mammaglobin was evident in adenoid cystic carcinoma. Positivity was observed on the luminal side of the cytoplasm of true ductal cells (original magnification ×20).*

mucinous type was positive in 2 (10.0%) of 20 cases, and the mucinous type was positive in 10 (25%) of 40 cases. In the nonlepidic growth type, the acinar-cribriform type was positive in 3 (15.0%) of 20 cases, and the solid type was negative in all cases.

Squamous Cell Carcinomas.—Mammaglobin expression was observed in only one case of moderately differentiated squamous cell carcinoma, but this positive area was restricted to a small part of the tumor (Figure 2, A). All other squamous cell carcinomas were negative for mammaglobin. All squamous cell carcinomas were immunonegative for GCDFP-15.

Pleomorphic Carcinoma.—In pleomorphic carcinomas, expression of GCDFP-15 was observed in 1 (5.0%) of 20 cases, whereas all cases were immunonegative for mammaglobin.

Neuroendocrine Tumors.—Expression of mammaglobin was observed in 1 (5.2%) of the 19 carcinoid tumors, but positivity was limited to a small area (Figure 2, B). Furthermore, expression of GCDFP-15 was observed in 1 different case (5.2%), but the positivity again was limited to a small area (Figure 2, C).

All high-grade neuroendocrine tumors (large-cell neuroendocrine carcinoma and small-cell carcinoma) were immunonegative for both mammaglobin and GCDFP-15.

Salivary Gland–Type Tumors (Mucoepidermoid Carcinoma and Adenoid Cystic Carcinoma) of the Bronchus and/or Trachea

In mucoepidermoid carcinomas, expression of GCDFP-15 was observed in 2 (40.0%) of 5 cases, whereas all cases were immunonegative for mammaglobin. In adenoid cystic carcinoma, 1 (9.1%) of 11 cases was immunopositive for mammaglobin, whereas all cases were immunonegative for GCDFP-15. Mammaglobin (Figure 2, C) and GCDFP-15 showed focal staining.

Malignant Mesotheliomas

All malignant mesotheliomas were immunonegative for both mammaglobin and GCDFP-15.

COMMENT

In the present study, we demonstrated 3 advantages of using mammaglobin over GCDFP-15 to identify breast carcinoma metastatic to the lung. The first advantage is that the sensitivity of mammaglobin is slightly higher than that of GCDFP-15. The mammaglobin positivity rate for primary breast cancer is reported to be between 47.9%[19] and 71%.[20] Although we focused on analyzing breast carcinoma metastatic to the lung, the overall prevalence of mammaglobin expression in our series (50%) is almost accordant with the findings of previous reports[19,20] on primary breast cancer. The expression status of some molecules may be altered between primary and metastatic lesions. For example, the expression of surfactant apoprotein in lung cancer is frequently reduced in metastatic sites.[21] However, a previous report has demonstrated that the concordance rate of mammaglobin expression between the primary site and lymph node metastases was 93%.[20] These findings indicate that mammaglobin expression is not altered in the metastatic lesion.

Several studies have analyzed the mammaglobin expression pattern in breast carcinoma using immunohistochemical methods. Two of three studies used a noncommercial antibody[15] or a cocktail of antibodies[20] to identify mammaglobin, and the positivity rate in primary breast carcinoma was around 70%. However, Sasaki et al[19] reported that the positivity rate for mammaglobin in primary breast carcinoma analyzed by commercially available monoclonal antibody (clone 304-1A5) was lower than that using a noncommercial antibody or a cocktail of antibodies. These findings suggest that commercially available monoclonal antibody has a lower sensitivity and that there might be differences in the patient population. According to analyses by histologic type, mammaglobin ex-

pression was reported to be higher in lobular carcinoma than in ductal carcinoma.[19,20] Another study has suggested that mammaglobin expression is evident mainly in well-differentiated hormone receptor–positive breast carcinomas.

The second advantage of using mammaglobin is that the immunopositive area shows more diffuse staining than that of GCDFP-15. Similar findings have also been reported by Bhargava et al.[20] These findings indicate that examination of mammaglobin expression would be advantageous when the diagnosis is based on a limited sample, such as biopsy material. However, as cases that are immunopositive for mammaglobin and GCDFP-15 are partly exclusive, the combined use of both markers is important.

The third advantage of using mammaglobin is that its expression was found in only 1.1% of nonbreast tumors of the lung and pleura. One carcinoid tumor, 1 squamous cell carcinoma, 1 adenoid cystic carcinoma of the trachea, and none of the primary lung adenocarcinomas were positive. In primary lung adenocarcinoma, about 30% of cases demonstrated a nonlepidic growth pattern.[22] In particular, the cribriform and/or acinar and solid type might be confused with a lung metastasis from breast cancer. In the present study, we demonstrated that mammaglobin was negative in the cribriform and/or acinar and solid types of primary lung adenocarcinoma. The mammaglobin expression rate in lung tumors is reported to range from 0% to 16.7%.[15,19,20,23] Mammaglobin expression was reported to have been found in 20% of salivary gland tumors.[15,20] Therefore, the finding that adenoid cystic carcinoma of the trachea showed immunoreactivity for mammaglobin is not surprising but does require attention.

The differential diagnosis of malignant effusion involving the serosal membrane may be difficult. In the present study, all malignant mesotheliomas were immunonegative for mammaglobin. These findings indicated that mammaglobin should be added as one of the mesothelioma-negative markers, especially in female patients and/or cases of peritoneal mesothelioma.

Thyroid transcription factor 1 (TTF-1) has been shown to play a crucial role in the morphogenesis and function of the lung by regulating gene expression of surfactant proteins.[24] Most studies have reported finding TTF-1 expression in more than 70% of primary adenocarcinomas of the lung.[25] Therefore, TTF-1 has been considered a reliable marker to distinguish between primary lung adenocarcinoma and metastatic adenocarcinoma. It is reasonable that TTF-1 should be added to the antibody panel as a negative marker for metastatic tumors.

In conclusion, we demonstrated that the sensitivity of mammaglobin is equal or superior to that of GCDFP-15 for investigation of breast carcinoma metastatic to the lung. Immunopositivity for mammaglobin is more diffuse than that for GCDFP-15. In terms of practical diagnosis, mammaglobin immunopositivity can serve as a differential marker of breast carcinoma and should be added to immunohistochemical panels.

We thank Sachiko Miura and Chizu Kina for their skillful technical assistance. This work was supported in part by a Grant-in-aid for Cancer Research (16-6) from the Ministry of Health, Welfare, and Labor of Japan.

References

1. Dail DH, Cagle PT, Marchevsky AM, et al. Metastases to the lung. In: Travis WD, Brambilla E, Muller-Hermelink HK, Harris CC, eds. *Pathology and Genetics of Tumours of the Lung, Pleura, Thymus and Heart.* Lyon, France: IARC Press; 2004:122–124. *World Health Organization Classification of Tumours.*

2. Hess KR, Varadhachary GR, Taylor SH, et al. Metastatic patterns in adenocarcinoma. *Cancer.* 2006;106:1624–1633.

3. Bejar J, Sabo E, Eldar S, Lev M, Misselevich I, Boss JH. The prognostic significance of the semiquantitatively determined estrogen receptor content of breast carcinomas: a clinicopathological study. *Pathol Res Pract.* 2002;198:455–460.

4. Lamy PJ, Pujol P, Thezenas S, et al. Progesterone receptor quantification as a strong prognostic determinant in postmenopausal breast cancer women under tamoxifen therapy. *Breast Cancer Res Treat.* 2002;76:65–71.

5. Kaufmann O, Deidesheimer T, Muehlenberg M, Deicke P, Dietel M. Immunohistochemical differentiation of metastatic breast carcinomas from metastatic adenocarcinomas of other common primary sites. *Histopathology.* 1996; 29:233–240.

6. Kaufmann O, Kother S, Dietel M. Use of antibodies against estrogen and progesterone receptors to identify metastatic breast and ovarian carcinomas by conventional immunohistochemical and tyramide signal amplification methods. *Mod Pathol.* 1998;11:357–363.

7. O'Connell FP, Wang HH, Odze RD. Utility of immunohistochemistry in distinguishing primary adenocarcinomas from metastatic breast carcinomas in the gastrointestinal tract. *Arch Pathol Lab Med.* 2005;129:338–347.

8. Tot T. The role of cytokeratins 20 and 7 and estrogen receptor analysis in separation of metastatic lobular carcinoma of the breast and metastatic signet ring cell carcinoma of the gastrointestinal tract. *APMIS.* 2000;108:467–472.

9. Raju U, Ma CK, Shaw A. Signet ring variant of lobular carcinoma of the breast: a clinicopathologic and immunohistochemical study. *Mod Pathol.* 1993; 6:516–520.

10. Di Nunno L, Larsson LG, Rinehart JJ, Beissner RS. Estrogen and progesterone receptors in non–small cell lung cancer in 248 consecutive patients who underwent surgical resection. *Arch Pathol Lab Med.* 2000;124:1467–1470.

11. Canver CC, Memoli VA, Vanderveer PL, Dingivan CA, Mentzer RM. Sex hormone receptors in non-small-cell lung cancer in human beings. *J Thorac Cardovasc Surg.* 1994;108:153–157.

12. Ishibashi H, Suzuki T, Suzuki S, et al. Progesterone receptor in non–small cell lung cancer—a potent prognostic factor and possible target for endocrine therapy. *Cancer Res.* 2005;65:6450–6458.

13. Chu P, Wu E, Weiss ML. Cytokeratin 7 and cytokeratin 20 expression in epithelial neoplasms: a survey of 435 cases. *Mod Pathol.* 2000;13:962–972.

14. Mark RW, Tamera JL, Gary TC, et al. Gross cystic disease fluid protein-15 as a marker for breast cancer: immunohistochemical analysis of 690 human neoplasms and comparison with alphalactalbumin. *Hum Pathol.* 1989;30:281–287.

15. Han JH, Kang Y, Shin HC, et al. Mammaglobin expression in lymph nodes is an important marker of metastatic breast carcinoma. *Arch Pathol Lab Med.* 2003;127:1330–1334.

16. Watson MA, Fleming TP. Isolation of differentially expressed sequence tags from human breast cancer. *Cancer Res.* 1994;54:4598–4602.

17. Watson MA, Darrow C, Zimonjic DB, et al. Structure and transcriptional regulation of the human mammaglobin gene, a breast cancer associated member of the uteroglobin gene family localized to chromosome 11q13. *Oncogene.* 1998;16:817–824.

18. Watson MA, Fleming TP. Mammaglobin, a mammary specific member of the uteroglobin gene family, is overexpressed in human breast cancer. *Cancer Res.* 1996;56:860–865.

19. Sasaki E, Tsunoda N, Hatanaka Y, et al. Breast-specific expression of MGB1/mammaglobin: an examination of 480 tumors from various organs and clinicopathological analysis of MGB1-positive breast cancers. *Mod Pathol.* 2007; 20:208–214.

20. Bhargava R, Beriwal S, Dabbs DJ. Mammaglobin vs GCDFP-15: an immunohistologic validation survey for sensitivity and specificity. *Am J Clin Pathol.* 2007;127:103–113.

21. Yatabe Y, Mitsudomi T, Takahashi T. TTF-1 expression in pulmonary adenocarcinomas. *Am J Surg Pathol.* 2002;26:767–773.

22. Aida S, Shimazaki H, Sato K, et al. Prognostic analysis of pulmonary adenocarcinoma subclassification with special consideration of papillary and bronchioloalveolar types. *Histopathology.* 2004;45:468–476.

23. Ciampa A, Fanger G, Khan A, et al. Mammaglobin and CRxA-01 in pleural effusion cytology: potential utility of distinguishing metastatic breast carcinomas from other cytokeratin 7-positive/cytokeratin 20-negative carcinomas. *Cancer.* 2004;102:368–372.

24. Fabbro D, Di Loreto C, Stamerra O, Beltrami CA, Lonigro R, Damante G. TTF-1 gene expression in human lung tumors. *Eur J Cancer.* 1996;32A:512–517.

25. Lau SK, Luthringer DJ, Eisen RN. Thyroid transcription factor-1: a review. *Appl Immunohistochem Mol Morphol.* 2002;10:97–102.

+Model
LUNG-2857; No. of Pages 7

Lung Cancer (2007) xxx, xxx–xxx

available at www.sciencedirect.com

ScienceDirect

journal homepage: www.elsevier.com/locate/lungcan

SHORT COMMUNICATION

Mucoepidermoid carcinoma of the lung: High-resolution CT and histopathologic findings in five cases

Taichiro Ishizumi[a,b,*], Ukihide Tateishi[a], Shun-ichi Watanabe[b], Yoshihiro Matsuno[c]

[a] *Divisions of Diagnostic Radiology and Nuclear Medicine, National Cancer Center Hospital, 5-1-1, Tsukiji, Chuo-Ku, 104-0045 Tokyo, Japan*
[b] *Divisions of Thoracic Surgery, National Cancer Center Hospital, 5-1-1, Tsukiji, Chuo-Ku, 104-0045 Tokyo, Japan*
[c] *Divisions of Pathology, National Cancer Center Hospital, 5-1-1, Tsukiji, Chuo-Ku, 104-0045 Tokyo, Japan*

Received 13 December 2006; received in revised form 30 June 2007; accepted 21 August 2007

KEYWORDS
Mucoepidermoid carcinoma;
Lung;
High-resolution CT

Summary
Objective: The purpose of this study was to characterize the high-resolution computed tomography (HRCT) findings of mucoepidermoid carcinoma of the lung and correlate them with the histopathological features.
Methods: The study included five patients with pathologically proven mucoepidermoid carcinoma who underwent HRCT before treatment. The HRCT findings were then compared with the histopathological features in all patients.
Results: The HRCT images showed lesions in the central lung in four patients and in the peripheral lung in one. All the lesions were well defined nodules or masses with a smooth margin. The contour of the tumours was oval ($n = 3$), round ($n = 1$) or lobulated ($n = 1$). The contrast-enhanced CT images showed marked heterogeneous enhancement with foci of relatively low attenuation in four of the five lesions and mild heterogeneous enhancement in the other lesion. There was an admixed distribution of areas that are heterogeneous in the densities of blood vessels, as highlighted by immunohistochemical staining of CD31. Most mucin-secreting areas of the tumours showed more densely distributed blood vessels, mostly capillaries, in between tumour cell nests, whereas other areas did less. All five patients in our series underwent lobectomy plus lymph node dissection or sampling. All the patients are alive without evidence of disease an average of 50.4 months after surgery (range, 15–82 months; median, 57 months).

* Corresponding author at: Divisions of Diagnostic Radiology and Nuclear Medicine, National Cancer Center Hospital, 5-1-1, Tsukiji, Chuo-Ku, 104-0045 Tokyo, Japan. Tel.: +81 3 3542 2511; fax: +81 3 3542 3815.
E-mail address: tishizumi@hotmail.co.jp (T. Ishizumi).

0169-5002/$ – see front matter
doi:10.1016/j.lungcan.2007.08.022

Please cite this article in press as: Ishizumi T, et al., Mucoepidermoid carcinoma of the lung: High-resolution CT and histopathologic findings in five cases, Lung Cancer (2007), doi:10.1016/j.lungcan.2007.08.022